

# Dielectric properties of $\text{Pb}(\text{Zn}_{1/3}, \text{Nb}_{2/3})\text{O}_3$ ceramics modified by $\text{Ba}(\text{Zn}_{1/3}, \text{Nb}_{2/3})\text{O}_3$ and $\text{BaTiO}_3$

J.-K. LEE

*Department of Materials Engineering, Chosun University, Kwangju 501-759, South Korea*

S.-G. KANG, H. KIM

*Department of Inorganic Materials Engineering, Seoul National University, Seoul 151-742, South Korea*

Dielectric properties of lead zinc niobate (PZN) ceramics modified by barium zinc niobate (BZN) and  $\text{BaTiO}_3$  (BT) were investigated. By adding the modifier of BT and BZN, the stabilization of perovskite phase of PZN increased, but its Curie temperature decreased linearly with the amount of added modifier. Room temperature dielectric constant of PZN increased by addition of stabilizers up to 12 and 15 mol% of BZN and BT, respectively. The maximum room temperature dielectric constant was observed to be 7800 at 12 mol% of BZN, and 9800 at 15 mol% of BT, respectively. © 1998 Chapman & Hall

## 1. Introduction

Lead-based ferroelectric relaxor materials of the form of  $\text{Pb}(\text{B}_1, \text{B}_2)\text{O}_3$  usually have high dielectric constants with a broad dielectric maxima. A number of relaxor materials can be sintered at relatively low temperature (about 1000 °C) compared with barium titanate-based systems, and they are promising candidate materials for capacitor, transducer, and micropositioner applications [1–6]. The low sintering temperature of relaxors is especially attractive to the capacitor industry since expensive platinum or palladium electrodes can be replaced with less expensive silver or silver–palladium electrodes [4–6].

Lead zinc niobate  $\text{Pb}(\text{Zn}_{1/3}, \text{Nb}_{2/3})\text{O}_3$  composition (PZN) compound is a relaxor ferroelectric with a perovskite structure exhibiting the diffuse phase transition [6–10]. It has a rhombohedral structure at room temperature and undergoes a phase transition at 140 °C to cubic structure. The solid solution between PZN with rhombohedral symmetry and  $\text{PbTiO}_3$  (PT) with tetragonal symmetry has a morphotropic phase boundary (MPB) at room temperature for a composition near 9 mol% of PT and the composition near the MPB show usually large dielectric and piezoelectric constants and higher electro-mechanical coupling coefficients (about 92%) than those of the PZT family ceramics [11–13].

It is well known that when the pure PZN or PZN–PT ceramics with the perovskite structure are prepared by conventional ceramic processing, the formation of pyrochlore phase invariably occurs [13–16]. The pyrochlore phase of the type  $\text{PbNb}_2\text{O}_6$  is detrimental to both dielectric and piezoelectric properties.

Halliyal [17–19] and Furukawa *et al.* [20] have reported that the formation of the pyrochlore phase in

PZN can be suppressed by adding 15 mol% of either  $\text{BaTiO}_3$  or  $\text{SrTiO}_3$ . They also explained that  $\text{BaTiO}_3$  (BT) or  $\text{SrTiO}_3$  stabilizes the perovskite structure in PZN because BT and  $\text{SrTiO}_3$  have higher electro-negativity difference and tolerance factor [17–20].

In the present study, stabilization of perovskite phase in PZN ceramics was undertaken by simultaneously adding only a small amount of a  $\text{BaTiO}_3$  and  $\text{Ba}(\text{Zn}_{1/3}, \text{Nb}_{2/3})\text{O}_3$  (denoted by BZN), and the phase relations and dielectric properties were investigated in PZN–BT–BZN ternary system.

## 2. Experimental procedure

In the pseudoternary system  $(1 - x - y)\text{PZN} - x\text{BT} - y\text{BZN}$ , compacts were prepared by conventional solid state sintering. Near PZN, compositions were selected at 1 mol% intervals to determine the minimum amount of BT, BTZN and BZN needed to form the ceramics with 100% perovskite phase. Reagent grade powders of  $\text{PbO}$ ,  $\text{ZnO}$ ,  $\text{Nb}_2\text{O}_3$ ,  $\text{TiO}_2$  and  $\text{BaCO}_3$  were used as starting materials. The constituents were dried prior to weighing. The mixtures were ball milled in polyethylene jars with ethanol for 12 to 16 h using zirconia grinding media. The slurry was dried and calcined at 900 °C for 2 h. The calcined powder was ball milled and dried again to enhance homogeneity. Pellets with 12 mm diameter and 2–3 mm thickness were pressed with PVA binder, and the binder was burnt out by a slow heating to and keeping at 500 °C for 1 h. Compacts were sintered in a sealed alumina crucible at 1100 and 1150 °C for 1 h, using a heating rate of 200 °C h<sup>-1</sup> in an SiC resistance furnace. To suppress  $\text{PbO}$  loss from the compacts, a  $\text{PbO}$ -rich atmosphere was maintained by placing an equimolar mixture of  $\text{PbO}$  and  $\text{ZrO}_2$  inside the crucible.

Powder X-ray diffractometry (PW 1700, Philips Electronic Co.) with  $\text{CuK}\alpha$  radiation used and the relative amounts of pyrochlore and perovskite phases were determined from the X-ray diffraction patterns of sintered bodies by measuring the major X-ray peak intensities for the perovskite and pyrochlore phases, for example (1 1 0) and (2 2 2), respectively. The percentage of perovskite phase was calculated from X-ray peak intensities using the following equation [2]

$$\% \text{ perovskite} = \frac{I_{\text{perovskite}}(110)}{I_{\text{perovskite}}(110) + I_{\text{pyrochlore}}(222)} \times 100 \quad (1)$$

Theoretical density was calculated from lattice parameter measurements, and bulk densities were geometrically determined. Grain size was measured from scanning electron microscope (SEM) micrographs.

For measurements of dielectric properties, gold electrodes were sputtered and air-drying silver paint was applied over gold electrodes. Dielectric properties were measured by an automated system, where temperature control box and LCR meter (HP4 192A) were controlled by a desktop computer. Dielectric constants and dissipation factors were measured between 1 and 100 kHz, as the samples were cooled at a rate of 3 to 4 °C min<sup>-1</sup>. The temperature range covered was 2 to 160 °C.

### 3. Results and discussion

#### 3.1. Properties of sintered body

The sintered density and percentage of perovskite phase of the compositions of (1 - x)PZN-xBTZN are given in Table I. Compositions with  $\geq 8$  mol % BTZN showed 100% perovskite phase, while a pyro-

TABLE I Sintering temperature, relative density, and per cent perovskite phase of (1 - x)PZN-xBTZN

x	Sintering temperature (°C)	Relative density (%)	Perovskite phase (%)
0.04	1100	90-91	70
0.05	1100	94-95	80
0.07	1100	94-95	94
0.08	1100	95-96	100
0.09	1100	95-96	100
0.10	1100	95-96	100
0.12	1150	94-96	100
0.14	1150	92-94	100
0.15	1150	92-94	100
0.20	1150	92-94	100

TABLE II Sintered density, grain size, and room temperature dielectric constant of 0.86PZN-0.14BTZN sintered at 1100 °C with variation of sintering time. Powder mixture was calcined at 900 °C for 2 h

Sintering time (h)	Average grain size (μm) <sup>a</sup>	Sintered density (g cm <sup>-3</sup> )	Dielectric constant (at 25 °C)
1	1.2	7.53	9000
2	2.2	7.70	9200
4	3.3	7.78	9600

<sup>a</sup>Measured by SEM.

chlore phase ( $\text{Pb}_3\text{Nb}_4\text{O}_{13}$ ) was observed in composition of 4 to 7 mol % BTZN. The amount of pyrochlore phase decreased with the amount of BTZN additive. Relative density of sintered body increased with BTZN additives and reached to about 95% of theoretical over 5 mol % BTZN addition. The relative densities were in the range of 95 to 96% for the specimens of 8 to 10 mol % BTZN with 100% perovskite phase.

Table II presents the grain size calculated by a linear intercept technique and the density of 0.86PZN-0.14BTZN ceramics sintered at 1100 °C for 1, 2 and 4 h. The average grain size increased from 1.2 to 2.2 μm with increasing the sintering time from 1 to 2 h. In this system, sintered density increased to 7.78 g cm<sup>-3</sup> until 4 h and then slowly decreased after 4 h, caused by PbO loss [21].

#### 3.2. Dielectric properties

The temperature dependence of dielectric constant (at 1 kHz) for a range of compositions are shown in Fig. 1. The magnitude of the dielectric constant maximum increased with the addition of up to 7 mol % BT and decreased with further addition, as shown in Fig. 1a. The maximum dielectric constants increased with the addition of 8 and 10 mol % of BTZN and BZN, respectively (Fig. 1b and c); after which, the maximum dielectric constants decreased. It should be noted that the maximum dielectric constants decrease, although the amount of perovskite phase were always 100%. The variation of Curie temperature with compositions is shown in Fig. 2. The Curie temperature decreased linearly with the addition of BaTiO<sub>3</sub>, BTZN, and BZN. For the compositions PZN containing 15 mol % BaTiO<sub>3</sub>, 14 mol % BTZN and 12 mol % BZN, respectively,  $T_{\text{max}}$  is about that of room temperature.

Fig. 3 shows the substitution dependence of the room temperature dielectric constants of PZN-BZN ceramics, which were sintered at 1100 °C for 4 h. The room temperature dielectric constants depend on the composition of BZN. The stabilizers increased the room temperature dielectric constants up to 12 and 15 mol % of BZN and BT, respectively. The composition dependence of the room temperature dielectric constants is shown in Fig. 4. The maximum room temperature dielectric constants were 7800 at 12 mol % of BZN, 9200 at 14 mol % BTZN, and 9800 at 15 mol % of BT.

An interesting result of this study is the apparent grain size dependence of dielectric constant. As listed in Table II, the dielectric constants of PZN-BTZN

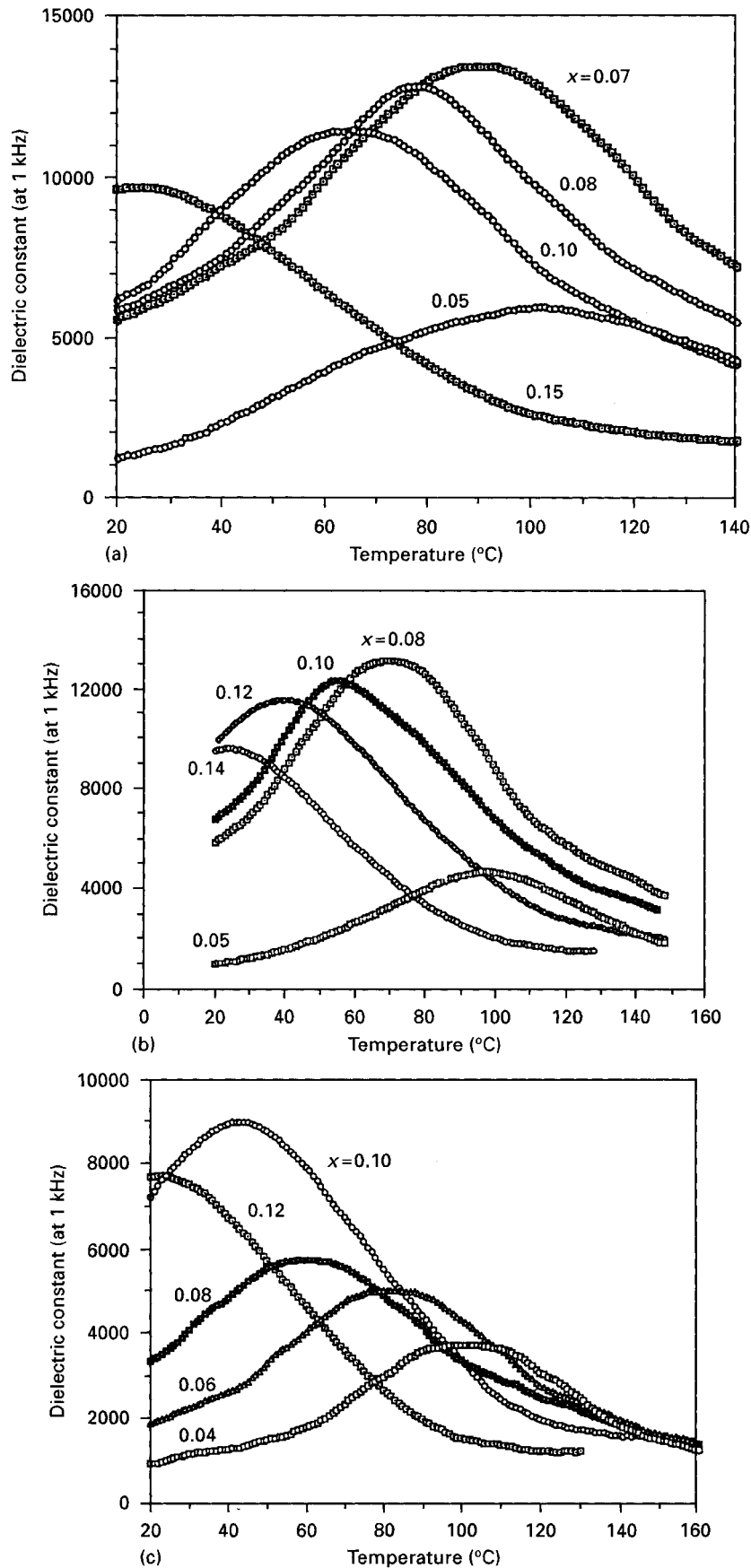


Figure 1 Dielectric constant with variation of temperature in (a)  $(1-x)\text{PZN}-x\text{BT}$ , (b)  $(1-x)\text{PZN}-x\text{BTZN}$  and (c)  $(1-x)\text{PZN}-x\text{BZN}$  ceramics sintered at  $1100^\circ\text{C}$  for 2 h.

increased with sintering time. In this composition, dielectric constant increased with sintering time until 16 h and then slowly decreased in specimen sintered for 32 h because of the density reduction caused by

PbO loss [21]. But the true grain-size effects on the dielectric constant cannot be resolved easily due to the difficulty in varying grain size without changing density, PbO loss, microcracking, etc.

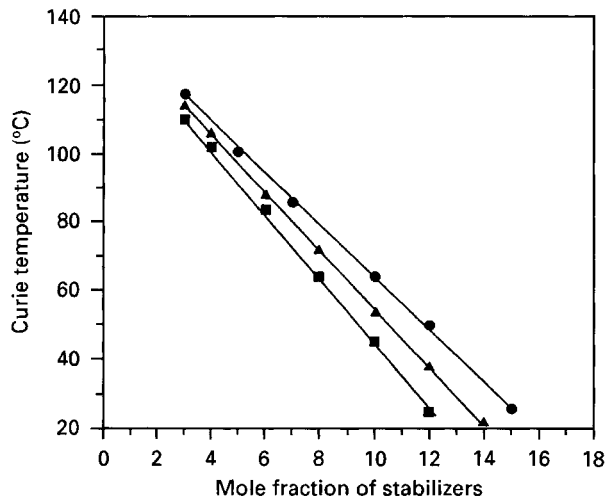


Figure 2 Variation of Curie temperature in stabilized PZN ceramics at 1 kHz with BT (●), BTZN (▲) and BZN (■).

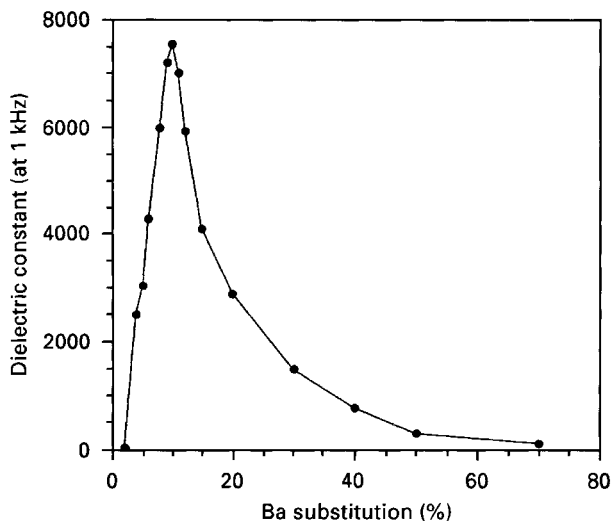


Figure 3 Room temperature dielectric constant (at 1 kHz) in  $(1-x)\text{PZN}-x\text{BZN}$  ceramics sintered at  $1100^\circ\text{C}$  for 2 h.

### 3.3. Diffuse phase transition

The compositions containing up to 70 mol % BTZN showed a diffuse phase transition and an a.c. frequency dependence of  $T_{\text{max}}$  (temperature of dielectric permittivity maximum). Fig. 5 shows the temperature dependence of dielectric constant at three different frequencies for a composition containing 8 mol % BTZN. All the compositions of this study showed broad maxima of dielectric constant and an increase in  $T_{\text{max}}$  with increasing a.c. frequency, showing the dielectric dispersion characteristics of relaxor ferroelectrics. Corresponding frequency dispersion of the dissipation factor was also observed. The temperature difference ( $\Delta T$ ) between the  $T_{\text{max}}$  measured at 1 and 100 kHz gives a rough estimate of the relaxor characteristics. The value of  $T_{\text{max}}$  are listed in Table III. As shown in Table III, the composition containing ~30 mol % BTZN showed the strongest frequency dispersion.

For ferroelectrics with a diffuse phase transition, the quadratic law has been shown to hold over a wide temperature range instead of the normal Curie-Weiss

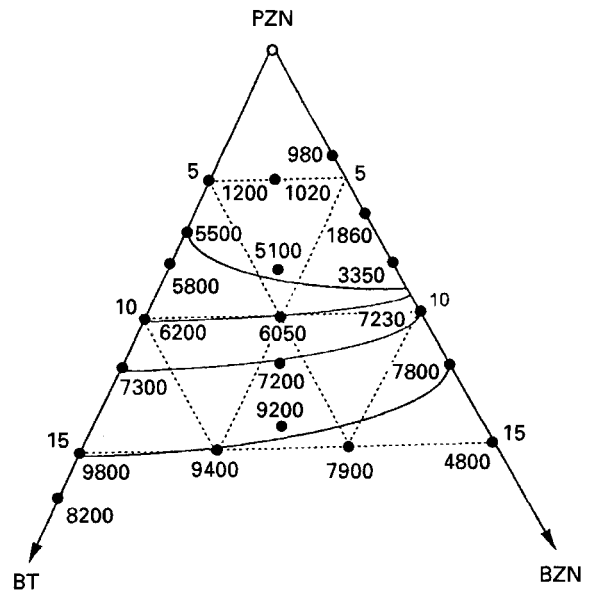


Figure 4 Room temperature dielectric constant (at 1 kHz) in  $(1-x-y)\text{PZN}-x\text{BZN}-y\text{BT}$  ceramics sintered at  $1100^\circ\text{C}$  for 2 h.

law. If the distribution of the local Curie temperature is Gaussian, the reciprocal permittivity ( $1/K$ ) can be approximated as follows

$$1/K = 1/K_{\text{max}} + (T - T_{\text{max}})^2 / (2K_{\text{max}} \delta^2) \quad (2)$$

where  $\delta$  is the diffuseness parameter, which is a measure of the dielectric dispersion or the diffuse phase transition (DPT). For PZN-BTZN compositions, the values of  $\delta$  were calculated from the slope of plots of  $1/K$  versus  $(T - T_{\text{max}})^2$  [22]. The estimated  $\delta$  showed an increase of  $\delta$  with the amount of BTZN and was highest for compositions with 30 to 60 mol % of BTZN, indicating a broadened phase transition for these compositions.

### 3.4. Temperature coefficient of capacitance

In the PZN-BT-BZN system, the composition with 15 mol % BT, 14 mol % BTZN, and 12 mol % BZN were investigated further as a potential capacitor material. They showed dielectric constant maxima at room temperature and showed the values of 7800-9800 and a dissipation factor of 2-4% at room temperature. The temperature coefficient of capacitance (denoted by TCC) is defined as follows

$$\text{TCC} = (C_T - C_{\text{RT}}) / C_{\text{RT}} \times 100 \quad (3)$$

where  $C_T$  and  $C_{\text{RT}}$  are the dielectric constants at temperature  $T$  and room temperature, respectively. TCC for 8 to 12 mol % BTZN compositions is shown in Fig. 6. The TCC curve is only slightly changed up to  $60^\circ\text{C}$  in case of 14 mol % BTZN. This point may be valuable for application of the compositions in the industry use.

### 3.5. Relaxor nature

The temperature dependence of dielectric constants of PZN-BTZN compositions showed that dielectric constant obeys the quadratic law above the transition

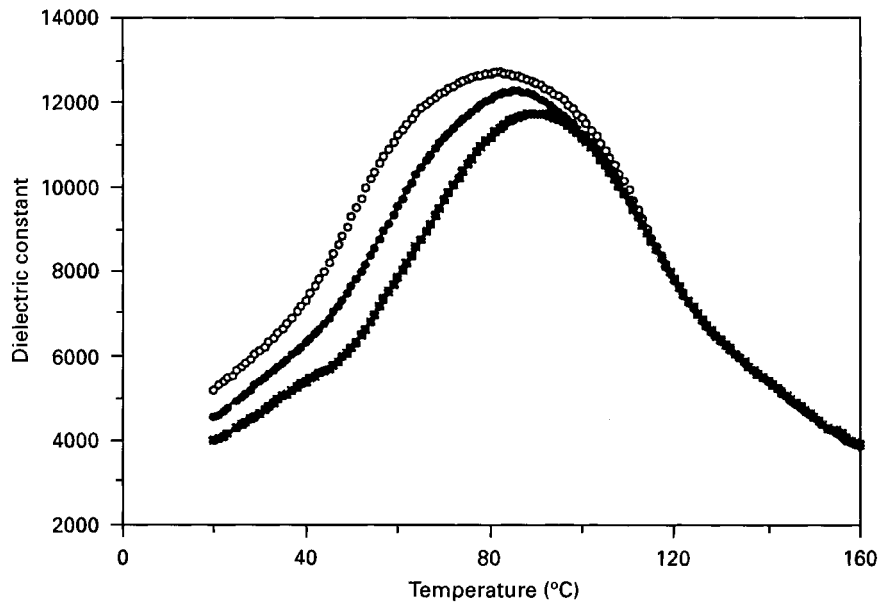


Figure 5 Effect of measuring frequency on the room temperature dielectric constant in 0.92PZN-0.08BTZN ceramics sintered at 1100 °C for 2 h. (○) 1 kHz; (●) 10 kHz; (■) 100 kHz.

TABLE III Dielectric properties of (1 - x)PZN-xBTZN ceramics

x	$\Delta T$ [ $T_{\max}$ (100 kHz) - $T_{\max}$ (1 kHz)] (°C)	$k_{\max}$ (1 kHz)	Diffused parameter, $\delta$ (°C)
0.05	7	5000	0
0.07	12	13 000	54
0.08	13	13 500	58
0.09	14	12 800	61
0.10	15	12 600	62
0.12	16	11 800	64
0.14	18	9200	70
0.20	21	7000	86
0.30	23	3400	95
0.40	22	2900	102
0.50	20	2200	104
0.60	18	1800	98
0.70	16	1700	80

temperature. For several compositions, the diffuseness parameter ( $\delta$ ) and the difference temperature ( $\Delta T$ ) between  $T_{\max}$  (1 kHz) and  $T_{\max}$  (100 kHz) increased with increasing the stabilizers, which indicates the enhancement of relaxor characteristics [19]. But a solid solution of PZN-BT was expected to show a transition temperature between 140 and 120 °C. This discrepancy could be explained by considering the compositions of individual unit cells. In these solid solutions the perovskite unit cells will be made of PZ, PN, PT, BZ, BN, or BT. That is, the individual components of the solid solution are the ferroelectric PZN, PT, BT and nonferroelectric BZN. Therefore, the components can be regarded as (1 - x - y - z) PZN-xBT-yPT-zBZN, as it is impossible to find the exact concentration of each component.

#### 4. Conclusions

The perovskite phase of PZN ceramics could be stabilized to 100% by the addition of more than 8 to 10 mol% of BTZN and its Curie temperature de-

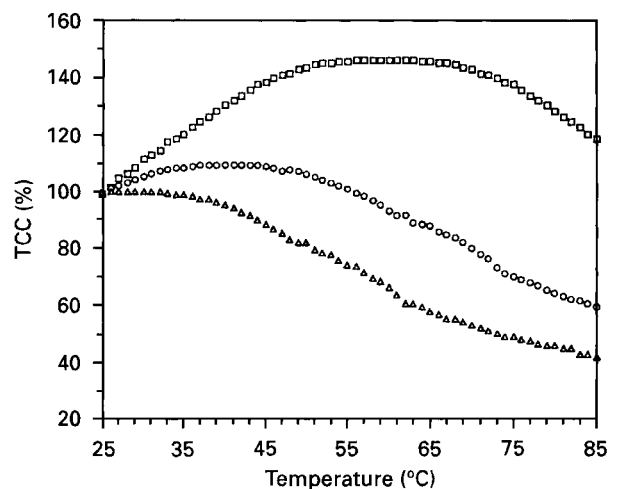


Figure 6 Temperature coefficients of capacitance in (1 - x)PZN-xBTZN ceramics sintered at 1100 °C for 2 h. (□) 0.08; (○) 0.12; (△) 0.14.

creased linearly with the additions of BT, BTZN, and BZN. For the compositions of PZN containing 15 mol% BT,  $T_c$  is approximately room temperature. Room temperature dielectric constants of PZN increased by addition of stabilizers up to 12 and 15 mol% of BZN and BT, respectively. Above these compositions, the dielectric constant at room temperature decreased with an increase of the amounts of stabilizers. The maximum room temperature dielectric constant was observed to be 7800 at 12 mol% of BZN, 9200 at 14 mol% of BTZN and 9800 at 15 mol% of BT, respectively. The temperature dependence of the dielectric constants showed a broad peak near to room temperature.

#### Acknowledgements

This study was supported (in part) by research funds from Chosun University 1997.

## References

1. T. R. SHROUT and A. HALLIVAL, *Amer. Ceram. Soc. Bull.* **66** (1987) 704.
2. S. L. SWARTZ and T. R. SHROUT, *Mater. Res. Bull.* **17** (1982) 1245.
3. Y. YOKOMIZO, T. TAKAHASHI and S. NOMURA, *J. Phys. Soc. Jpn* **28** (1970) 1278.
4. G. E. HAERTING, "Electronic ceramics" (Marcell Dekker Inc., New York, 1988) p. 371.
5. J. M. HAUSSONNE, G. DESGARDIN, P. BAJOLET and B. RAUEAN, *J. Amer. Ceram. Soc.* **66** (1983) 801.
6. V. A. BOKOV and I. E. MYL'NICOVA, *Sov. Phys. Solid State (English Translation)* **3** (1961) 613.
7. S. L. SWARTZ, T. R. SHROUT, W. A. SCHULZE and L. E. CROSS, *J. Amer. Ceram. Soc.* **67** (1984) 311.
8. S. NOMURA, J. KUWATA, S. J. JANG, L. E. CROSS and R. E. NEWNHAM, *Mater. Res. Bull.* **14** (1979) 769.
9. Y. YOKOMIZO, T. TAKAHASHI and S. NOMURA, *J. Phys. Soc. Jpn* **28** (1970) 1278.
10. S. NOMURA, H. ARIMA and F. KOJIMA, *Jpn J. Appl. Phys.* **12** (1973) 531.
11. J. KUWATA, K. UCHINO and S. NOMURA, *ibid.* **21** (1981) 1298.
12. T. R. GURURAJA, A. SAFARI and A. HALLIYAL, *Amer. Ceram. Soc. Bull.* **65** (1986) 1601.
13. J. BELSICK, A. HALLIYAL, U. KUMAR and R. E. NEWNHAM, *J. Amer. Ceram. Soc.* **66** (1987) 664.
14. H. C. LING, M. F. YAN and W. W. RHODES, *J. Mater. Sci.* **24** (1989) 541.
15. S. NOMURA, M. ENDO and F. KOJIMA, *Jpn J. Appl. Phys.* **13** (1974) 2004.
16. J. KUWATA, K. UCHINO and S. NOMURA, *Ferroelectrics* **22** (1979) 863.
17. A. HALLIYAL, U. KUMAR, R. E. NEWNHAM and L. E. CROSS, *J. Amer. Ceram. Soc.* **70** (1987) 119.
18. A. HALLIYAL, U. KUMAR, R. E. NEWNHAM and L. E. CROSS, *Amer. Ceram. Soc. Bull.* **66** (1987) 671.
19. T. R. SHROUT and A. HALLIYAL, *ibid.* **66** (1987) 704.
20. O. FURUKAWA, Y. YAMASHITA, M. HARATA, T. TAKAHASHI and K. IGARASHI, *J. Appl. Phys.* **23-24** (1985) 96.
21. S. G. KANG, J. K. LEE and H. KIM, unpublished work.
22. S. M. PILGRIM, A. E. SUTERLAND and S. R. WINZER, *J. Amer. Ceram. Soc.* **73** (1990) 3122.

*Received 20 September 1996  
and accepted 5 August 1997*